

Showcasing research from Professors Naoki Aratani and Hiroko Yamada's laboratory, Division of Materials Science, Nara Institute of Science and Technology (NAIST), Ikoma, Japan.

A remarkably strained cyclo-1,8-pyrenylene trimer that undergoes metal-free direct oxygen insertion into the biaryl C–C  $\sigma$ -bond

A remarkably strained cyclo-1,8-pyrenylene trimer was synthesized and it underwent the first biaryl C–C  $\sigma$ -bond cleavage by direct oxygen insertion without the aid of any metal agents at room temperature. A priori highly strained cyclo-1,8-pyrenylene trimer exhibits the longest wavelength emission among all pyrene-based fluorophores due to the intensive electronic interactions between pyrenes. A vivid color change of fluorescence from orange to light blue is observed upon oxidation. This strain-induced transformation could be also applied for sulfur atom insertion into a biaryl  $\sigma$ -bond.

### As featured in:



See Naoki Aratani,  
Hiroko Yamada et al.,  
*Chem. Sci.*, 2019, **10**, 6785.


 Cite this: *Chem. Sci.*, 2019, **10**, 6785

All publication charges for this article have been paid for by the Royal Society of Chemistry

 Received 11th April 2019  
 Accepted 11th June 2019

 DOI: 10.1039/c9sc01777a  
[rsc.li/chemical-science](http://rsc.li/chemical-science)

## Introduction

Cycloarylenes such as cycloparaphenylenes (CPPs) have attracted interest due to their unique structure, remarkable physical properties, and potential applications in materials science.<sup>1–4</sup> The remarkable characteristics of CPPs are often derived from their curved  $\pi$ -conjugated systems. Recently, Yamago and co-workers reported two C–C  $\sigma$ -bond cleavages of [5]- and [6]-CPPs with a platinum salt<sup>5</sup> driven by their internal strain energy<sup>6</sup> (the values are significantly higher than those of cyclopropane).<sup>7</sup> In organic chemistry, a molecule experiences strain when the molecule is held in an energetically unfavorable conformation by intramolecular covalent bonds in comparison to a strain-free reference compound.<sup>8</sup> After cutting off the particular bonds, the strain energy would be released. Ring strain is a type of instability that results from a combination of angle strain (Baeyer strain), torsional strain (Pitzer strain), and transannular strain known as van der Waals (or Prelog) strain.<sup>9</sup> Angle strain occurs to achieve maximum bond strength in a specific conformation in which the bond angles deviate from

the ideal bond angles. The potential energy and unique bonding structure present in the molecules with ring strain can be used to drive reactions in organic synthesis. Examples of such reactions are small ring opening reactions, photo-induced ring opening of cyclobutenes and nucleophilic ring-opening of epoxides.<sup>10–12</sup> Strain-induced C–C bond activation with transition metals has been long known.<sup>13</sup> As another type of example, spherical  $sp^2$  carbons in fullerenes tend to react as electrophiles.<sup>14</sup> The driving force is the release of strain when double bonds become saturated.

Here we report the synthesis and reactivity of a remarkably strained cyclopyrenylene trimer **CP3** (Scheme 1). Since the first synthesis of diphenylethers by Cook in 1901,<sup>15</sup> almost all biaryl ether syntheses so far developed have relied on the Williamson-type nucleophilic aromatic substitution. The only exceptions are the metal-mediated oxidation reactions of biphenylenes (Scheme 1).<sup>11</sup> In this work, direct oxygen atom insertion into a biaryl C–C  $\sigma$ -bond is achieved for the first time under ambient conditions without any aid of metal agents.

## Results and discussion

### Synthesis and structural characterization

Macrocyclic arylene **CP3** was synthesized by a Ni-mediated coupling reaction of 1,8-dibromo-4,5-dipropoxypyrene<sup>16</sup> according to reported procedures.<sup>17–19</sup> We performed a one-pot macrocyclization reaction of the dibromopyrene with  $Ni(cod)_2$ /2,2'-bipyridine in a mixture of toluene and DMF (76.0 mM). **CP3** was successfully isolated from higher oligomers using silica gel and gel permeation chromatography in 3.5% yield.

High-resolution matrix-assisted-laser-desorption/ionization spiral time-of-flight mass spectroscopy (HR-MALDI-TOF-MS) detected the parent ion peak at  $m/z = 948.4384$  (calcd for

<sup>a</sup>Division of Materials Science, Nara Institute of Science and Technology (NAIST), 8916-5 Takayama-cho, Ikoma, Nara 630-0192, Japan. E-mail: aratani@ms.naist.jp; hyamada@ms.naist.jp

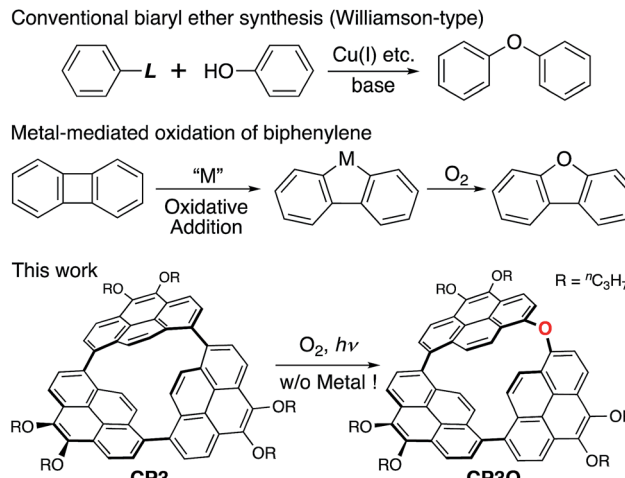
<sup>b</sup>Department of Material and Life Science, Division of Advanced Science and Biotechnology, Graduate School of Engineering, Osaka University, 2-1 Yamadaoka, Suita, Osaka 565-0871, Japan

<sup>c</sup>Institute for Research Initiatives, Division for Research Strategy, NAIST, 8916-5 Takayama-cho, Ikoma, Nara 630-0192, Japan

<sup>d</sup>Data Science Center, NAIST, 8916-5 Takayama-cho, Ikoma, Nara 630-0192, Japan

<sup>†</sup> Electronic supplementary information (ESI) available: Detailed experimental procedures, characterization of molecules and additional spectroscopic computational data. CCDC 1907392 and 1907393. For ESI and crystallographic data in CIF or other electronic format see DOI: 10.1039/c9sc01777a





**Scheme 1** General biaryl ether synthesis, metal-mediated oxidation of a biphenylene, and direct oxygen insertion into a highly strained C–C  $\sigma$ -bond.

$C_{66}H_{60}O_6 = 948.4383$  [M]<sup>+</sup>). The  $^1H$  NMR spectrum of **CP3** in  $CDCl_3$  reveals only a single set of signals that consists of one singlet peak at 6.99 ppm due to protons at the 9,10-positions and two doublet peaks at 8.60 and 8.67 ppm due to protons at the 2,7- and 3,6-positions, respectively. These data indicate that the cyclic pyrene **CP3** adopts a  $D_{3h}$  symmetric structure in solution.

The structure of **CP3** has been unambiguously revealed by X-ray diffraction analysis.<sup>20</sup> The smoothly curved pyrene 1 and pyrene 3 in Fig. 1a were held with a small torsion angle (19.5(6) $^\circ$ ), which stands in marked contrast to conventional perpendicular 1,1'-linked pyrene dimers.<sup>21</sup> The  $\pi$ -orbital axis vector (POAV) angles, the degree of the pyramidalization of trigonal carbon atoms,<sup>22</sup> were calculated based on the crystal structure (Fig. 1b). Two of the largest POAV values (4.88 $^\circ$  and 4.04 $^\circ$ ) were found at C(1) and C(54) atoms, respectively, but these angle strains are not as high as those of C<sub>60</sub> (11.64 $^\circ$ ) and [6]CPP (6.10 $^\circ$ ).<sup>23</sup> It is noticed that the C(1)–C(54) bond length of the curved bipyrene unit is 1.546(5)  $\text{\AA}$ , being distinctly longer than that of the normal C<sub>Ar</sub>–C<sub>Ar</sub> bond (av. 1.49  $\text{\AA}$ ).<sup>24</sup> Surprisingly, the distance between C(13) and C(56) atoms (10,10'-positions) of the coplanar bipyrene is 2.88  $\text{\AA}$ , much shorter than the sum of van der Waals radii of carbon atoms (*ca.* 3.40  $\text{\AA}$ ), thus resulting in the negative Gaussian curvature<sup>25</sup> of two encountered six-membered rings with transannular strain (Fig. 1b). In total, the ring strain affects the elongation of the C(1)–C(54)  $\sigma$ -bond. The conformation of the coplanar bipyrene unit has the same shape as a rotational transition state of binaphthyl *via* the *syn*-Cs form,<sup>26</sup> letting us easily imagine its high energy state.

## Photophysical properties

**CP3** absorbs UV-vis light with an absorption maximum at 505 nm, and emits fluorescence at 599 nm with a quantum yield of  $\Phi_F = 0.34$  at 298 K along with a small short wavelength emission (*vide infra*) (Fig. 2). Curiously, this red-shifted emission of **CP3** is much longer than that of the pyrene excimer ( $\lambda_{\text{max}}$

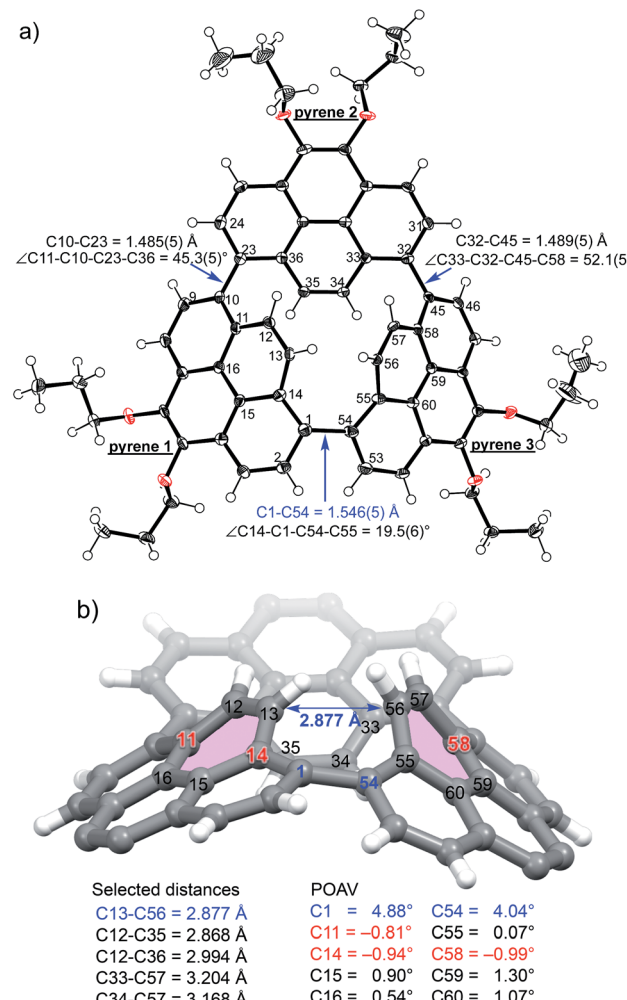


**Fig. 1** Single crystal X-ray structure of **CP3** and selected distances, angles and POAV values. (a) ORTEP drawing (50% probability) of the top view and (b) ball-and-stick model of the side view. Two six-membered rings with negative Gaussian curvature are shown in pink.

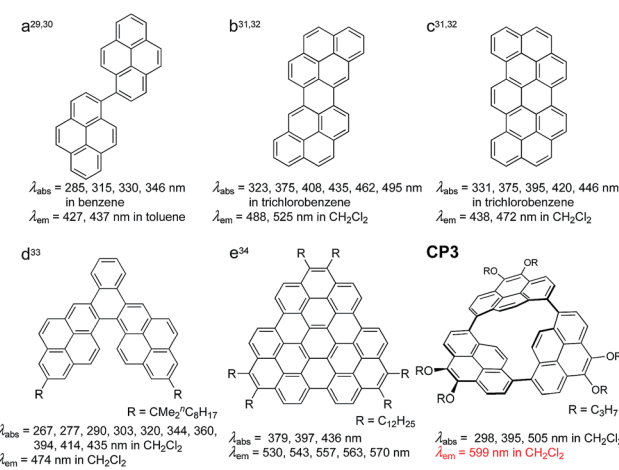


Chart 1



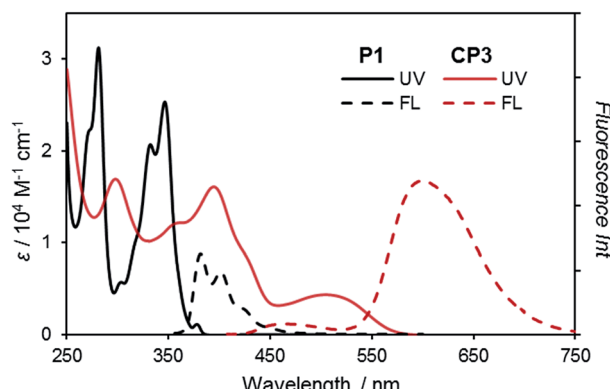


Fig. 2 (a) UV-vis (solid line) and fluorescence (broken line) spectra of CP3 (in red) along with those of 4,5-dipropoxypyrene (P1) (in black) in  $\text{CH}_2\text{Cl}_2$ ,  $[\text{CP3}] = 1.5 \times 10^{-5}$  M. Fluorescence spectra were recorded for excitation ( $\lambda_{\text{ex}} = 346$  nm for P1,  $\lambda_{\text{ex}} = 395$  nm for CP3) with the absorbance adjusted to 0.1.

$= 475$  nm in hexane)<sup>27,28</sup> and any fused pyrene dimers ( $\lambda_{\text{max}} =$  up to 525 nm; Chart 1b-d).<sup>29-33</sup> Most importantly, this is even longer than that of the completely fused corresponding pyrene trimer ( $\lambda_{\text{max}} = 530$ -570 nm, Chart 1e).<sup>34</sup> To the best of our knowledge, this is the most red-shifted emission among all pyrene-based fluorophores besides acetylene-linked cyclic trimers and tetramers.<sup>16</sup> These properties result from the intensive electronic interaction between pyrene units in the highly strained structure.

### DFT calculations

To further understand these unusual electronic features, density functional theory (DFT) and time-dependent (TD)-DFT calculations both at the B3LYP-D3/6-311G(d,p)//B3LYP-D3/6-31G(d) level including the SMD solvation model with a dielectric constant of dichloromethane were carried out (Fig. 3 and the computational details are provided in the ESI†).<sup>35</sup> The highest occupied molecular orbital (HOMO) and lowest unoccupied molecular orbital (LUMO) are non-degenerative and the coefficient distribution in these frontier MOs appears delocalized over pyrenes 1 and 3. The longest band of CP3 at 548 nm mainly comprises the transition from high HOMO ( $-5.00$  eV) to low LUMO ( $-2.37$  eV) relative to a linear pyrene trimer P3 (HOMO:  $-5.31$  eV, LUMO:  $-1.89$  eV, Fig. S20†) with the oscillator strength,  $f = 0.279$ . The red-shifted absorption and emission were predominantly achieved by the stabilized LUMO relative to P3, which is caused by the  $\pi^*$ - $\pi^*$  conjugation between C(13) and C(56) atoms. The transition energies and oscillator strengths simulated by TD-DFT showed good agreement with the observed absorption spectrum (Fig. S18†).

### C-C $\sigma$ -bond cleavage by oxidation

Meanwhile, we found that the short wavelength emission gradually enhanced under ambient conditions. We measured fluorescence spectral changes under room light in  $\text{CH}_2\text{Cl}_2$  (Fig. 4). The fluorescence of CP3 clearly indicates a new peak at 480 nm with the isosbestic point at 553 nm, from which a 1 : 1

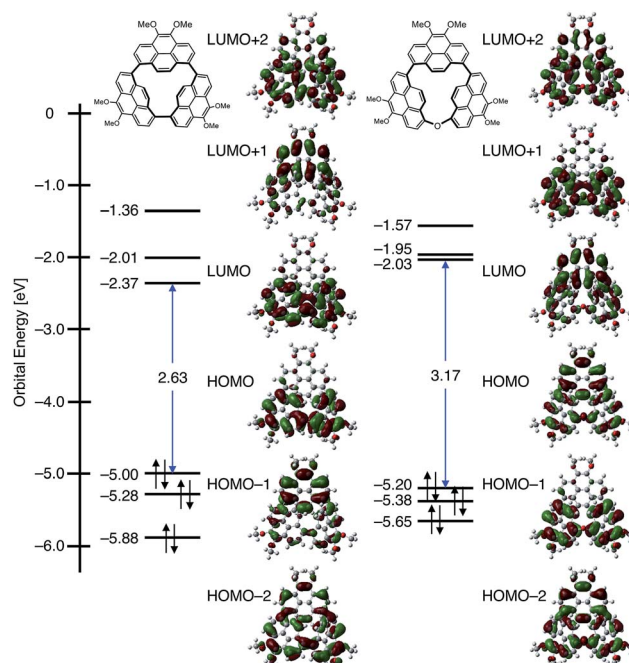


Fig. 3 MO diagrams of CP3 and CP3O based on calculations at the B3LYP-D3/6-311G(d,p)//B3LYP-D3/6-31G(d) including the SMD solvation model. Propyl groups were replaced by Me groups.

transformation was expected. The color of the emission drastically changes from orange to light blue (Fig. 4 inset). From the time profile, we have determined the half lifetime to be 18 h.

After 78 h, CP3 was completely transformed. The structure of the product was initially characterized by  $^1\text{H}$  NMR spectroscopy. In the  $^1\text{H}$  NMR spectrum, 9 peaks in the aromatic region appear and the protons at the 10,10'-positions of the coplanar pyrene rings are significantly deshielded from  $\delta = 6.99$  ppm to 8.90 ppm as a doublet ( $\text{d}, J = 10.0$  Hz). All these spectra are consistent with the product having  $C_{2v}$  symmetry, lowering from  $D_{3h}$ . HR-MALDI-TOF-MS of the product detected a CP3 +

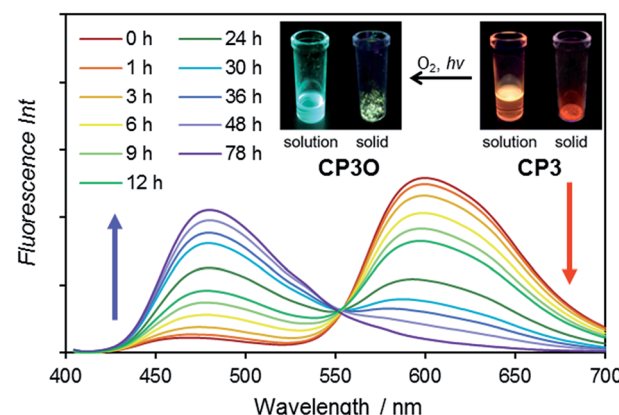


Fig. 4 Fluorescence spectral change of CP3 under room light in  $\text{CH}_2\text{Cl}_2$ . Insets are photos of the solution ( $\text{CH}_2\text{Cl}_2$ ) and solid of CP3 and CP3O under UV irradiation.

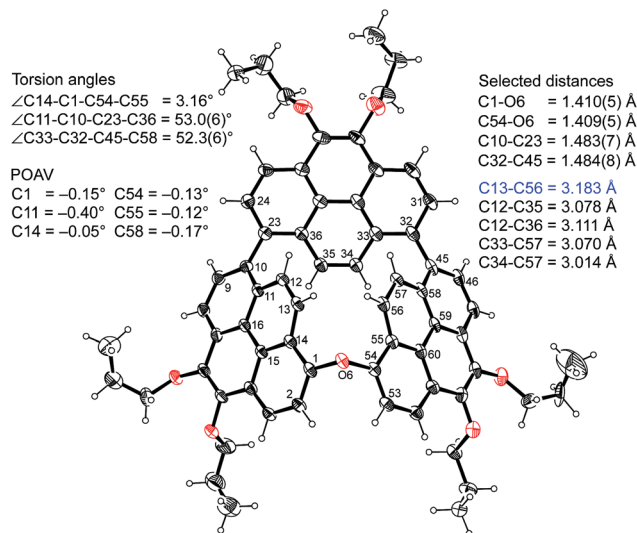
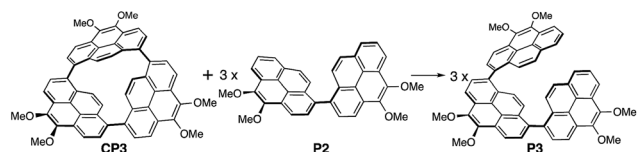


Fig. 5 Single crystal X-ray structure and selected distances, angles and POAV values of **CP3O**. The thermal ellipsoids are shown at 25% probability. One of the two identical molecules in the crystallographic asymmetric unit of **CP3O** is shown.



Scheme 2 A hypothetical homodesmotic reaction for the calculation of strain energies of **CP3**. Propyl groups were replaced by Me groups.

16 mass unit at  $m/z = 964.4347$  (calcd for  $C_{66}H_{60}O_7 = 964.4334$   $[M]^+$ ), suggesting the insertion of one oxygen atom.

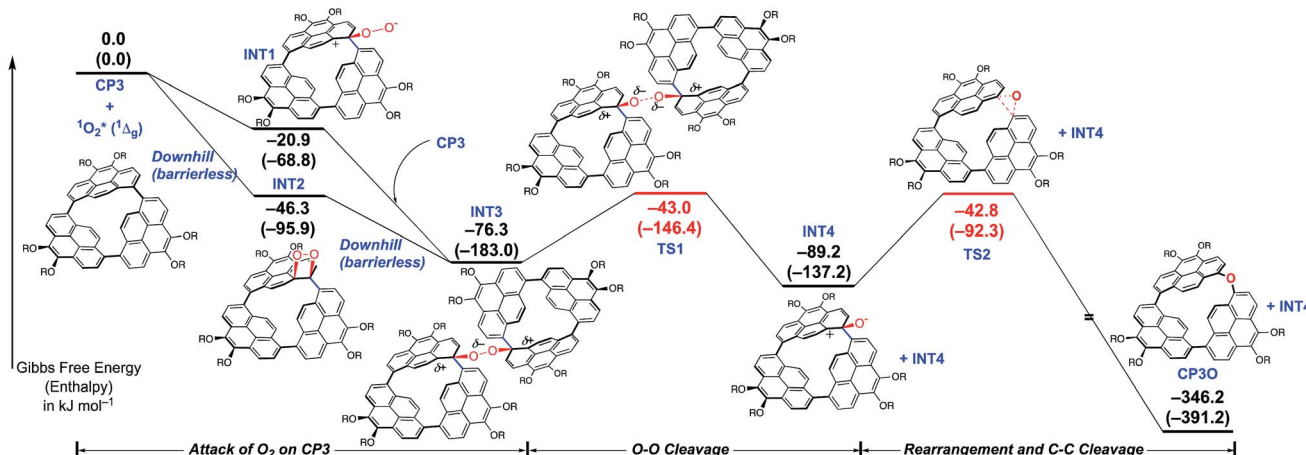
The structure was finally determined by single crystal X-ray diffraction analysis (Fig. 5).<sup>20</sup> The product has an arched structure with an oxygen atom between two pyrenes, thus

revealing that the cyclic ether **CP3O** was quantitatively formed.<sup>36</sup> All the structural parameters suggested that the ring strain is no longer involved, predicted from the atom–atom distances and torsion angles (Fig. 5). The larger dihedral angles make the electronic interactions between pyrenes weak, resulting in a blue-shifted absorption and emission spectra with  $\Phi_F = 0.54$ . The reaction is sensitive to the solvent and proceeded smoothly in  $CH_2Cl_2$  and  $CHCl_3$ . We confirmed that the oxygen atom originates from molecular oxygen by reacting in  $H_2^{18}O$  saturated  $CH_2Cl_2$  to generate **CP3<sup>16</sup>O**. No C–C bond activation occurred without light, thus indicating that  $^1O_2^* ({}^1\Delta_g)$  reacts with **CP3**. To confirm the presence of singlet  $O_2$  derived from the excitation of **CP3**, we performed singlet  $O_2$  sensitization and measured the emission signal ( $\lambda_{em} = 1274$  nm) upon selective excitation of **CP3** at  $\lambda_{ex} = 515$  nm in  $O_2$ -saturated  $CH_2Cl_2$  (Fig. S17†). The quantum yield of singlet oxygen production ( $\Phi_\Delta$ ) determined with respect to  $\Phi_\Delta = 0.60$  for tetraphenylporphyrin (TPP)<sup>37</sup> is 0.33 at 298 K. Although the pyrene monomer is known as an efficient sensitizer for  $O_2$  with high  $\Phi_\Delta$ ,<sup>38</sup> it can absorb only UV light (Fig. 2). The absorption spectrum of **CP3** shows red-shifted broad bands up to *ca.* 600 nm, so the singlet  $O_2$  could be generated by room light.

The strain energy of **CP3** has been estimated on the basis of a homodesmotic reaction using **CP3**, dimer **P2**, and trimer **P3** (Scheme 2).<sup>38</sup> By using the heat of formation ( $\Delta H$ ) of the optimized structures of **CP3**, **P2**, and **P3**, the strain energy of **CP3** was obtained as 251 kJ mol<sup>-1</sup> (Fig. S20†). This is a higher strain energy per unit in comparison to [7]CPP.<sup>39</sup>

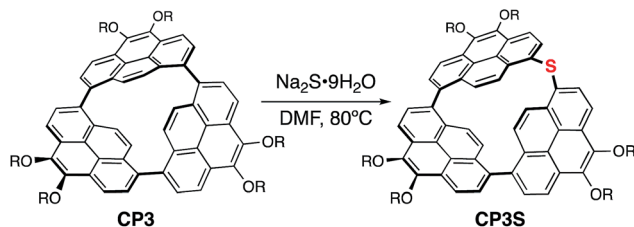
### Investigation of the reaction mechanism by DFT calculations

To elucidate the mechanism of C–C activation of **CP3**, the reaction pathway starting from **CP3** and a singlet oxygen molecule was explored using an automated reaction path search method, called the artificial force induced reaction (AFIR) method, combined with the DFT level of theory. As shown in Scheme 3, the bond formation between C(1) (or C(54) in Fig. 1)



Scheme 3 Gibbs free energy profile ( $\Delta G$  in  $kJ mol^{-1}$ ) of the formation of **CP3O** starting from **CP3** and a singlet oxygen molecule. The enthalpy differences are shown in parentheses. Propyl groups were replaced by Me groups. All the calculations were carried out at the B3LYP-D3/6-311G(d,p)//B3LYP-D3/6-31G(d) level including the SMD solvation model. Computational details and geometries are shown in the ESI.†





Scheme 4 Sulfur atom insertion into the C–C  $\sigma$ -bond of CP3. R =  $n$ C<sub>3</sub>H<sub>7</sub>.

and oxygen took place without a barrier to form intermediates **INT1** or **INT2**, followed by C–O bond formation with another CP3 affording **INT3**. As shown in Fig. S22 and S23,<sup>†</sup> the negative charge localized on the peroxide moiety in **INT3** caused the partial occupancy of the  $\sigma^*$  orbital of the peroxide moiety, which induced the decrease of the O–O bond order, *i.e.* O–O bond cleavage. After the formation of two neutral intermediates, **INT4**, the intramolecular rearrangement proceeded *via* a three-center transition state, which afforded the final product CP3O. The high exothermicity could be attributed to the release of strain upon transformation from **INT4** to CP3O.

### C–C $\sigma$ -bond cleavage by sulfidation

Finally, the transformation of CP3 into a cyclic thioether was also examined by using Na<sub>2</sub>S·9H<sub>2</sub>O as a reagent (Scheme 4). Treatment of CP3 with Na<sub>2</sub>S·9H<sub>2</sub>O in DMF at 80 °C for 72 h gave a sulfur inserted cyclic trimer CP3S in 67% conversion yield. CP3S exhibits light green emission with  $\Phi_F = 0.44$ . This is also the first direct sulfidation of a biaryl C–C  $\sigma$ -bond.<sup>36</sup> Synthesis of biaryl thioethers is considered as a valuable C–C bond activation process because transformations of diaryl sulfides and sulfones to the corresponding biaryl compounds have been developed.<sup>40</sup>

## Conclusions

In summary, we could isolate a highly strained cyclic pyrene trimer that underwent direct etherification at room temperature. This is the first example of biaryl C–C  $\sigma$ -bond cleavage under metal-free conditions. Because CP3 is the most bathochromic pyrene, a vivid color change of fluorescence is observed upon oxidation, being advantageous for the use of CP3 as a fluorescence probe for the imaging of singlet O<sub>2</sub> with relatively high  $\Phi_F$ .<sup>41</sup> We revealed that this unusual reactivity originates from the intense intramolecular energy in the highly strained structure. Besides, recently, O-doping of polycyclic aromatic hydrocarbons (PAHs) is emerging as a powerful strategy to tailor the optoelectronic properties of  $\pi$ -conjugated molecular modules.<sup>42</sup> This study presents a new concept for the preparation of potential sensing agents and O-doped PAHs. We would insert other elements into CP3 by which the optical and electronic properties can be controlled. Such possibilities are now under investigation and will be reported in due course.

## Conflicts of interest

There are no conflicts to declare.

## Acknowledgements

This work was partly supported by the Japan Society for the Promotion of Science (JSPS) KAKENHI Grant No. JP18K14190 (H. H.), JP18K14298 (M. S.), JP17H06445 (M. H.), JP17H03042 (N. A.) and JP26105004 (H. Y.). We thank Prof. A. Osuka (Kyoto Univ.) and Prof. K. Mizuno (NAIST) for fruitful discussion and, Profs. T. Kawai and T. Nakashima (NAIST) for measurements of fluorescence quantum yields and Ms Y. Nishikawa for MS measurements. We also acknowledge the computer resources provided by the Academic Center for Computing and Media Studies (ACCMS) at Kyoto University.

## Notes and references

- 1 S. Toyota and E. Tsurumaki, *Chem.–Eur. J.*, 2019, **25**, 6878–6890.
- 2 M. Iyoda and H. Shimizu, *Chem. Soc. Rev.*, 2015, **44**, 6411–6424.
- 3 X. Lu, S. Lee, Y. Hong, H. Phan, T. Y. Gopalakrishna, T. S. Herring, T. Tanaka, M. E. Sandoval, W. Zeng, J. Ding, D. Casanova, A. Osuka, D. Kim and J. Wu, *J. Am. Chem. Soc.*, 2017, **139**, 13173–13183.
- 4 M. A. Majewski and M. Stępień, *Angew. Chem., Int. Ed.*, 2019, **58**, 86–116.
- 5 E. Kayahara, T. Hayashi, K. Takeuchi, F. Ozawa, K. Ashida, S. Ogoshi and S. Yamago, *Angew. Chem., Int. Ed.*, 2018, **57**, 11418–11421.
- 6 T. Iwamoto, Y. Watanabe, Y. Sakamoto, T. Suzuki and S. Yamago, *J. Am. Chem. Soc.*, 2011, **133**, 8354–8361.
- 7 S. W. Benson, F. R. Cruickshank, D. M. Golden, G. R. Haugen, H. E. O’Neal, A. S. Rodgers, R. Shaw and R. Walsh, *Chem. Rev.*, 1969, **69**, 279–324.
- 8 K. B. Wiberg, *Angew. Chem., Int. Ed. Engl.*, 1986, **25**, 312–322.
- 9 E. V. Anslyn and D. A. Dougherty, in *Modern Physical Organic Chemistry, Chapter 2: Strain and Stability*, University Science Books, Sausalito, California, 2006, pp. 100–109.
- 10 A. Greenberg and J. F. Liebman, in *Strained Organic Molecules*, ed. H. H. Wasserman, Academic Press, 1st edn, 1978, vol. 38.
- 11 L. Souillart and N. Cramer, *Chem. Rev.*, 2015, **115**, 9410–9464.
- 12 G. Fumagalli, S. Stanton and J. F. Bower, *Chem. Rev.*, 2017, **117**, 9404–9432.
- 13 M. Murakami and N. Chatani, in *Cleavage of Carbon–Carbon Single Bonds by Transition Metals*, Wiley-VCH, Weinheim, 2015.
- 14 M. Prato, V. Lucchini, M. Maggini, E. Stimpfl, G. Scorrano, M. Eiermann, T. Suzuki and F. Wudl, *J. Am. Chem. Soc.*, 1993, **115**, 8479–8480.
- 15 A. N. Cook, *J. Am. Chem. Soc.*, 1901, **23**, 806–813.



16 G. Venkataramana, P. Dongare, L. N. Dawe, D. W. Thompson, Y. Zhao and G. J. Bodwell, *Org. Lett.*, 2011, **13**, 2240–2243.

17 T. Yamamoto, *Prog. Polym. Sci.*, 1992, **17**, 1153–1205; T. Yamamoto, Y. Hayashi and A. Yamamoto, *Bull. Chem. Soc. Jpn.*, 1978, **51**, 2091–2097.

18 J. Y. Xue, K. Ikemoto, N. Takahashi, T. Izumi, H. Taka, H. Kita, S. Sato and H. Isobe, *J. Org. Chem.*, 2014, **79**, 9735–9739.

19 Y. Yamamoto, E. Tsurumaki, K. Wakamatsu and S. Toyota, *Angew. Chem., Int. Ed.*, 2018, **57**, 8199–8202.

20 **CP3**:  $C_{66}H_{60}O_6$ ,  $M_w = 3493.9$ , triclinic, space group  $P\bar{1}$  (no. 2),  $a = 8.9771(10)$ ,  $b = 17.626(2)$ ,  $c = 17.763(2)$  Å,  $\alpha = 116.5169(19)$ ,  $\beta = 93.784(2)$ ,  $\gamma = 102.495(2)^\circ$ ,  $V = 2412.5(5)$  Å<sup>3</sup>,  $Z = 2$ ,  $T = 90(2)$  K,  $D_{\text{calcd}} = 1.307$  g cm<sup>−3</sup>,  $R_1 = 0.0738$  ( $I > 2\sigma(I)$ ),  $R_w = 0.2024$  (all data), GOF = 1.061. **CP3O**:  $C_{66}H_{60}O_7$  (methanol)<sub>0.59</sub> (dichloromethane)<sub>0.39</sub>,  $M_w = 1012.83$ , triclinic, space group  $P\bar{1}$  (no. 2),  $a = 17.7176(19)$ ,  $b = 18.088(2)$ ,  $c = 18.855(2)$  Å,  $\alpha = 109.8071(19)$ ,  $\beta = 114.3435(19)$ ,  $\gamma = 91.189(2)^\circ$ ,  $V = 5088.2(10)$  Å<sup>3</sup>,  $Z = 4$ ,  $T = 90(2)$  K,  $D_{\text{calcd}} = 1.322$  g cm<sup>−3</sup>,  $R_1 = 0.0829$  ( $I > 2\sigma(I)$ ),  $R_w = 0.2715$  (all data), GOF = 1.025. CCDC 1907392 and 1907393 contain the supplementary crystallographic data for this paper.

21 A. Matsumoto, M. Suzuki, H. Hayashi, D. Kuzuhara, J. Yuasa, T. Kawai, N. Aratani and H. Yamada, *Bull. Chem. Soc. Jpn.*, 2017, **90**, 667–677.

22 R. C. Haddon and L. T. Scott, *Pure Appl. Chem.*, 1986, **58**, 137–142; R. C. Haddon, *J. Am. Chem. Soc.*, 1987, **109**, 1676–1685; R. C. Haddon, *J. Phys. Chem.*, 1987, **91**, 3719–3720; R. C. Haddon, *Science*, 1993, **261**, 1545–1550.

23 Y. Segawa, A. Yagi, H. Ito and K. Itami, *Org. Lett.*, 2016, **18**, 1430–1433.

24 F. H. Allen, D. G. Watson, L. Brammer, A. G. Orpen and R. Taylor, in *International Tables for Crystallography*, ed. E. Prince, International Union of Crystallography, 2006, vol. C, ch. 9.5, pp. 790–811.

25 S. H. Pun and Q. Miao, *Acc. Chem. Res.*, 2018, **51**, 1630–1642.

26 L. Meca, D. Řeha and Z. Havlas, *J. Org. Chem.*, 2003, **68**, 5677–5680.

27 Th. Förster and K. Kasper, *Z. Phys. Chem.*, 1954, **1**, 275–277.

28 J. B. Birks, in *Photophysics of Aromatic Molecules*, Wiley, London, 1970, pp. 300–371.

29 V. A. Nefedov, *Russ. J. Org. Chem.*, 2007, **43**, 1163–1166.

30 R. A. Velapoldi, *J. Res. Natl. Bur. Stand., Sect. A*, 1972, **76**, 641–654.

31 E. Clar and O. Kühn, *Liebigs Ann.*, 1956, **601**, 181–192.

32 S. A. Tucker, A. I. Zvaigzne, W. E. Acree Jr, J. C. Fetzer and M. Zander, *Appl. Spectrosc.*, 1991, **45**, 424–428.

33 K.-i. Yamashita, A. Nakamura, Md. A. Hossain, K. Hirabayashi, T. Shimizu and K.-i. Sugiura, *Bull. Chem. Soc. Jpn.*, 2015, **88**, 1083–1085, Sugiura's dimer has  $\pi$ -conjugative planar bipyrene and emits at 474 nm, so the long wavelength emission of **CP3** originates from its highly strained structure. See text.

34 M. Kastler, J. Schmidt, W. Pisula, D. Sebastiani and K. Müllen, *J. Am. Chem. Soc.*, 2006, **128**, 9526–9534.

35 M. J. Frisch, G. W. Trucks, H. B. Schlegel, G. E. Scuseria, M. A. Robb, J. R. Cheeseman, G. Scalmani, V. Barone, B. Mennucci, G. A. Petersson, H. Nakatsuji, M. Caricato, X. Li, H. P. Hratchian, A. F. Izmaylov, J. Bloino, G. Zheng, J. L. Sonnenberg, M. Hada, M. Ehara, K. Toyota, R. Fukuda, J. Hasegawa, M. Ishida, T. Nakajima, Y. Honda, O. Kitao, H. Nakai, T. Vreven, J. A. Montgomery Jr, J. E. Peralta, F. Ogliaro, M. Bearpark, J. J. Heyd, E. Brothers, K. N. Kudin, V. N. Staroverov, R. Kobayashi, J. Normand, K. Raghavachari, A. Rendell, J. C. Burant, S. S. Iyengar, J. Tomasi, M. Cossi, N. Rega, J. M. Millam, M. Klene, J. E. Knox, J. B. Cross, V. Bakken, C. Adamo, J. Jaramillo, R. Gomperts, R. E. Stratmann, O. Yazyev, A. J. Austin, R. Cammi, C. Pomelli, J. W. Ochterski, R. L. Martin, K. Morokuma, V. G. Zakrzewski, G. A. Voth, P. Salvador, J. J. Dannenberg, S. Dapprich, A. D. Daniels, O. Farkas, J. B. Foresman, J. V. Ortiz, J. Cioslowski and D. J. Fox, *Gaussian 09, Revision E.1*, Gaussian, Inc., Wallingford CT, 2009.

36 Aromatization-driven oxygen and sulfur insertion reactions into a norcorrole (cyclic dipyrin dimer) were reported. T. Ito, Y. Hayashi, S. Shimizu, J.-Y. Shin, N. Kobayashi and H. Shinokubo, *Angew. Chem., Int. Ed.*, 2012, **51**, 8542–8545.

37 D. Yao, V. Hugues, M. Blanchard-Desce, O. Mongin, C. O. Paul-Roth and F. Paul, *New J. Chem.*, 2015, **39**, 7730–7733.

38 K. L. Marsh and B. Stevens, *J. Phys. Chem.*, 1983, **87**, 1765–1768.

39 Y. Segawa, H. Omachi and K. Itami, *Org. Lett.*, 2010, **12**, 2262–2265.

40 K. Nogi and H. Yorimitsu, *Chem. Commun.*, 2017, **53**, 4055–4065.

41 S. Kim, T. Tachikawa, M. Fujitsuka and T. Majima, *J. Am. Chem. Soc.*, 2014, **136**, 11707–11715.

42 Y. Wang, S. Qiu, S. Xie, L. Zhou, Y. Hong, J. Chang, J. Wu and Z. Zeng, *J. Am. Chem. Soc.*, 2019, **141**, 2169–2176; A. Berezin, N. Biot, T. Battisti and D. Bonifazi, *Angew. Chem., Int. Ed.*, 2018, **57**, 8942–8946; D. Stassen, N. Demitri and D. Bonifazi, *Angew. Chem., Int. Ed.*, 2016, **55**, 5947–5951; K. Nakanishi, D. Fukatsu, K. Takaishi, T. Tsuji, K. Uenaka, K. Kuramochi, T. Kawabata and K. Tsubaki, *J. Am. Chem. Soc.*, 2014, **136**, 7101–7109; K. Nakanishi, T. Sasamori, K. Kuramochi, N. Tokitoh, T. Kawabata and K. Tsubaki, *J. Org. Chem.*, 2014, **79**, 2625–2631.

